the benzyl ligand to a particular metal center, e.g. the η^2-CH_2Ph structure in **1a** versus the η^3-$CH_2C_6H_4$-*p*-Me group in its valence isoelectronic analogue, $CpMo(CO)_2(\eta^3$-$CH_2C_6H_4$-*p*-Me). On the basis of the similarities of the solid-state molecular structures possessed by complexes **1a**, **1b**, and **2**, it seems that steric effects play only a minor role in determining the mode of linkage of the unique benzyl ligand. Indeed, the propensity to attach benzyl ligands in an η^2 manner appears to be a general property of this class of compounds, since a variety of other Cp'M(NO)X(η^2-CH_2Ph) complexes (Cp' = Cp or Cp*; M = Mo or W; X = alkyl or halide) display this structural feature.[41] Nevertheless, while the valence-bond resonance forms provided earlier in this paper represent a reasonable description of the M-η^2-benzyl bonding in complexes **1a**, **1b**, **2**, **3**, and **4**, they do not provide a rationale for why the benzyl ligands in these compounds do not coordinate in an η^3 fashion to the metal centers and undergo the characteristic σ-π electronic distortion found for the allyl ligands in the related $CpW(NO)(\eta^3$-allyl)X compounds.[42]

Acknowledgment. We are grateful to the Natural Sciences and Engineering Research Council of Canada for support of this work in the form of grants to P.L., J.T., and F.W.B.E. We also thank Drs. C. A. Fyfe and H. Gies of this department for recording the ^{13}C CP/MAS solid-state NMR spectra of the bis(benzyl) complexes **1a**, **1b**, **2**, **3**, and **4**.

Supplementary Material Available: Tables of anisotropic thermal parameters for the non-hydrogen atoms and positional and thermal parameters for the hydrogen atoms of **1a**, **1b**, **2**, **3**, and **4** and tables of bond lengths and bond angles involving the hydrogen atoms for **1a**, **1b**, **2**, and **4** (27 pages); listings of observed and calculated structure factors for all the complexes (105 pages). Ordering information is given on any current masthead page.

(41) Dryden, N. H.; Legzdins, P. Manuscript in preparation.

(42) Greenhough, T. J.; Legzdins, P.; Martin, D. T.; Trotter, J. *Inorg. Chem.* **1979**, *18*, 3268 and references cited therein.

Thermolysis of $Cp^*Rh\{(\eta^4:\eta^1$-$C_4Me_4S)Fe(CO)_4\}$: A Case Study in Thiophene Desulfurization

Shifang Luo, Ann E. Ogilvy, Thomas B. Rauchfuss,* Arnold L. Rheingold,† and Scott R. Wilson

School of Chemical Sciences, University of Illinois, Urbana, Illinois 61801, and Department of Chemistry, University of Delaware, Newark, Delaware 19711

Received September 11, 1990

$Cp^*Rh(\eta^4$-$C_4Me_4S)$ (**1**) and $Fe_3(CO)_{12}$ react to give the ferrole $Cp^*Rh\{\eta^5$-$C_4Me_4Fe(CO)_3\}$ (**3**) together with trace amounts of $Cp^*Rh\{(\eta^4:\eta^1$-$C_4Me_4S)Fe(CO)_4\}$ (**2**). Compound **2** was prepared in high yield by the reaction of **1** with $Fe(CO)_5$ in the presence of Me_3NO. Thermolysis of **2** in refluxing toluene gave **3**, free C_4Me_4S (tetramethylthiophene, TMT), and $(Cp^*Rh)_2(\mu$-$CO)(\mu_3$-$S)Fe(CO)_3$ (**4**) in ca. 2:2:1 molar ratio. The efficiency of the conversion of **2** to **3** increased with added $Fe_3(CO)_{12}$ concomitant with the diminution of the yield for **4**. Control experiments showed that **3** and **4** are stable to $Fe_3(CO)_{12}$ in refluxing toluene. Furthermore, by labeling both the rhodium, with C_5Me_4Et, and the thiophene, as C_4Me_4S-*3,4-d*$_2$, we showed that the Rh-C_4Me_4S moiety remains intact during its desulfurization. The structures of **2**-**4** were determined by single-crystal X-ray diffraction. The desulfurization process illustrates the following mechanistic points: (i) transition metals play a dual role in thiophene desulfurization by separately stabilizing the desulfurized hydrocarbon and accepting the sulfur, (ii) the hydrocarbon is stabilized in the form of a metallacycle that structurally resembles thiophene, and (iii) the hydrocarbon and sulfide are stabilized in heterometallic environments.

Introduction

The coordination chemistry of thiophenes is of recent interest[1] because of its relevance to the metal-catalyzed hydrodesulfurization of fossil fuels.[2,3] The connection between coordination chemistry and thiophene desulfurization was first demonstrated by the research groups of Stone at Harvard and Markó at Veszprém. The former study showed that thiophene reacts with $Fe_3(CO)_{12}$ to give the ferrole $Fe_2C_4H_4(CO)_6$.[4] Subsequent work demonstrated that this reaction proceeded via thiaferroles $Fe_2SC_4R_4(CO)_6$, which convert to ferroles with the elimination of an insoluble iron sulfide (eq 1).[5] Markó and co-workers showed that thiophenes react with $Co_2(CO)_8$ to give $Co_2FeS(CO)_9$ under high pressures of hydrogen and

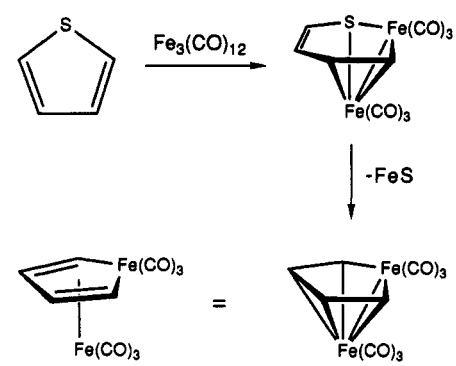

(1)

* To whom correspondence should be addressed at the University of Illinois.

† University of Delaware.

0276-7333/91/2310-1002$02.50/0

carbon monoxide. The iron was extracted from the walls of the autoclave, and the fate of the hydrocarbons was not determined.[6] It is noteworthy that in these model systems the desulfurization is effected by low-valent metal centers.

Recent work on molecular models for thiophene desulfurization has focused on the reactions of well-defined thiophene complexes. Most thiophene complexes exhibit no tendency to undergo C–S cleavage. C–S cleavage has been shown to occur upon 2e reduction of iridium(III) thiophene complexes[7] and by the reaction between 16e rhodium(I) centers and thiophenes.[8] The high reactivity of the recently reported η^4-thiophene complexes[9] suggested that they might be susceptible to desulfurization. Indeed, our preliminary studies showed that Cp*Rh(η^4-C_4Me_4S) reacts with $Fe_3(CO)_{12}$ to give the heterometallic ferrole Cp*Rh{η^5-$C_4Me_4Fe(CO)_3$}.[9a] The present report describes the isolation, characterization, and thermolysis of an intermediate in this desulfurization reaction.

In this study we use tetramethylthiophene (C_4Me_4S, TMT) as a model substrate. Our choice of this thiophene was guided both by experimental convenience and by its validity as a model substrate. Permethylation confers kinetic and thermodynamic stability to the resulting thiophene complexes.[10] For example, [Cp*Rh(η^5-C_4Me_4S)]$^{2+}$ is sufficiently robust that its solutions can be handled freely in air. With respect to the validity of C_4Me_4S as a model substrate, alkylthiophenes are more prevalent in fossil fuels than thiophene itself.[11] C_4Me_4S itself has been isolated from petroleum distillates.[12]

Results

Preparation of Cp*Rh(η^4-C_4Me_4S) (1). The reduction of [Cp*Rh(η^5-C_4Me_4S)]$^{2+}$ to Cp*Rh(η^4-C_4Me_4S) (1) by Cp_2Co proceeds in 85% yield (eq 2). The coproduct, $[Cp_2Co][OSO_2CF_3]$, is easily separated from 1 because of its poor solubility in nonpolar solvents. The 300-MHz ^{1}H NMR spectrum of 1 consists of three peaks, one for $C_5(CH_3)_5$ and two for η^4-$C_4(CH_3)_4S$ (Table I). The spectrum is invariant from +30 to −80 °C. High symmetry is also indicated by its ^{13}C NMR spectrum. The Cp* and C_4Me_4S ring carbon ^{13}C NMR resonances, all of which show ^{103}Rh–^{13}C coupling, appear at 121.7, 118.0, and 110.4 ppm for $[1]^{2+}$ and at 94.6, 88.4, and 42.8 ppm for 1. Heteronuclear chemical shift correlation techniques combined with isotopic labeling of the 3,4-methyl groups as CH_2D had previously been used to demonstrate that the most upfield ring carbon resonance originates from the 2,5-carbon atoms, i.e., those adjacent to sulfur.

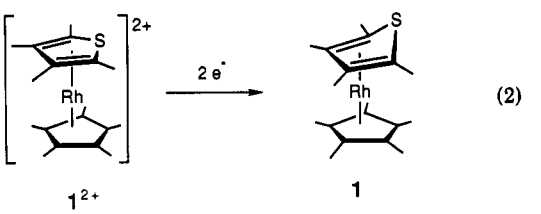

1^{2+} 1 (2)

Preparation and Structure of Cp*Rh{(η^4:η^1-C_4Me_4S)Fe(CO)$_4$} (2). The reaction of 1 with $Fe_3(CO)_{12}$ in refluxing toluene gives the yellow ferrole complex Cp*Rh{η^5-$C_4Me_4Fe(CO)_3$} (3) as the major product in 37% yield. In the workup of this reaction we occasionally obtained small amounts of the yellow compound Cp*Rh{(η^4:η^1-C_4Me_4S)Fe(CO)$_4$} (2). An improved procedure for the synthesis of 2 involves the Me_3NO-promoted reaction of $Fe(CO)_5$ with 1 (eq 3).

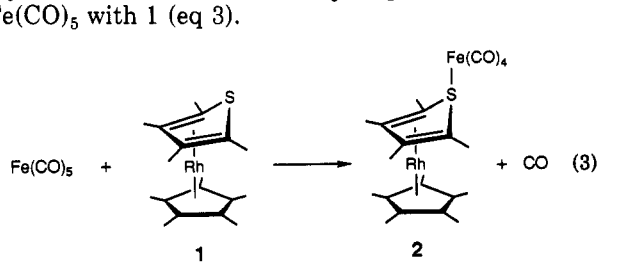

1 2 (3)

The 300-MHz ^{1}H NMR spectrum of 2 has three peaks: two for η^4-$C_4(CH_3)_4S$ and one for $C_5(CH_3)_5$ (Table I). The three ring ^{13}C NMR resonances all show coupling to the rhodium center. As seen in 1, one of the thiophene ring

Table I. ^{1}H and ^{13}C NMR Data for New Compounds

compd (solvent)	^{1}H, ppm		^{13}C, ppm (J(^{103}Rh,^{13}C), Hz)	
	Cp*	TMT	Cp*	TMT
$[1]^{2+}$ (CD_3COCD_3)	2.24	2.64 (2,5-Me)	110.71 (8.1)	122.07 (unresol)
		2.43 (3,4-Me)	12.56	118.30 (6.8)
				10.97
				9.68
1 (CD_3COCD_3)	1.71	1.98 (3,4-Me)	94.58 (6.2)	88.43 (7.3)
		1.13 (2,5-Me)	9.50	42.87 (14.8)
				15.25
				11.31
2 (C_6D_6)	1.30	1.57 (3,4-Me)	94.79 (6.3)	90.26 (6.6)
		1.23 (2,5-Me)	9.00	52.74 (15.2)
				12.33
				10.69
3 (CD_3COCD_3)	1.43	2.29 (2,5-Me)	97.13 (7.3)	167.62 (18.3)
		1.31 (3,4-Me)	9.80	113.16 (unresol)
				28.50
				12.30
4 (C_6D_6)	1.71			

(1) For developments before 1988, see: Angelici, R. J. *Acc. Chem. Res.* **1988**, *21*, 387. Some recent advances are reported in: (a) Lockemeyer, J. R.; Rauchfuss, T. B.; Rheingold, A. L.; Wilson, S. R. *J. Am. Chem. Soc.* **1989**, *111*, 8828. (b) Ganja, E. A.; Rauchfuss, T. B.; Wilson, S. R. *Organometallics* **1991**, *10*, 270. (c) Cordone, R.; Harman, W. D.; Taube, H. *J. Am. Chem. Soc.* **1989**, *111*, 5969. (d) Chaudret, B.; Jalón, F.; Pérez-Manrique, M.; Lahoz, F.; Plou, F. J.; Sánchez-Delgado, R. *New J. Chem.* **1990**, *14*, 331. (e) Chen, J.; Angelici, R. J. *Organometallics* **1990**, *9*, 879. (f) Latos-Grażyński, L.; Lisowski, J.; Olmstead, M. M.; Balch, A. L. *Inorg. Chem* **1989**, *28*, 1183. (g) Constable, E. C.; Henney, R. P. G.; Tocher, D. A. *J. Chem. Soc., Chem. Commun.* **1989**, 913.

(2) Gates, B. C.; Katzer, J. R.; Schuit, G. C. A. *Chemistry of Catalytic Processes*; McGraw-Hill: New York, 1979.

(3) Surface science studies: (a) Lang, J. L.; Masel, R. L. *Surf. Sci.* **1987**, *183*, 44. (b) Roberts, J. T.; Friend, C. M. *Surf. Sci.* **1987**, *186*, 201. (c) Gentle, T. M.; Tsai, C. T.; Walley, K. P.; Gellman, A. J. *Catal. Lett.* **1989**, *2*, 19. (d) Chianelli, R. R. *Catal. Rev.—Sci. Eng.* **1984**, *26*, 361. (e) Gellman, A. J.; Farias, M. H.; Somorjai, G. A. *J. Catal.* **1984**, *88*, 546. (f) Gellman, A. J.; Neiman, D.; Somorjai, G. A. *J. Catal.* **1987**, *107*, 92. (g) Bussell, M. E.; Somorjai, G. A. *J. Catal.* **1987**, *106*, 93. (h) Gellman, A. J.; Bussell, M. E.; Somorjai, G. A. *J. Catal.* **1987**, *107*, 103. (i) Stöhr, J.; Gland, J. L.; Kollin, E. B.; Koester, R. J.; Johnson, A. L.; Muetterties, E. L.; Sette, F. *Phys. Rev. Lett.* **1984**, *53*, 2161. (J) Zonnevylle, M. C.; Hoffmann, R.; Harris, S. *Surf. Sci.* **1988**, *199*, 320.

(4) (a) Kaesz, H. D.; King, R. B.; Manuel, T. A.; Nichols, L. D.; Stone, F. G. A. *J. Am. Chem. Soc.* **1960**, *82*, 4749. (b) King, R. B.; Treichel, P. M.; Stone, F. G. A. *J. Am. Chem. Soc.* **1961**, *83*, 3600. King, R. B.; Stone, F. G. A. *J. Am. Chem. Soc.* **1961**, *83*, 4557.

(5) (a) Manuel, T. A.; Meyer, T. J. *Inorg. Chem.* **1964**, *3*, 1049. (b) LeBorgne, G.; Grandjean, D. *Acta Crystallogr.* **1977**, *B33*, 344. (c) Hübener, P.; Weiss, E. *J. Organomet. Chem*, **1977**, *129*, 105. (d) Ogilvy, A. E.; Draganjac, M.; Rauchfuss, T. B.; Wilson, S. R. *Organometallics* **1988**, *7*, 1171.

(6) Markó, L. *Gazz. Chim. Ital.* **1979**, *102*, 247. (b) Khattab, S. A.; Markó, L.; Bor, G.; Markó, B. *J. Organomet. Chem.* **1964**, *1*, 373.

(7) Chen, J.; Daniels, L. M.; Angelici, R. J. *J. Am. Chem. Soc.* **1990**, *112*, 199.

(8) Jones, W. D.; Dong, L. *J. Am. Chem. Soc.* **1991**, *113*, 559.

(9) (a) Ogilvy, A. E.; Skaugset, A. E.; Rauchfuss, T. B. *Organometallics* **1989**, *8*, 2739. (b) Chen, J.; Angelici, R. J. *Organometallics* **1989**, *8*, 2277.

(10) Hachgenei, J. W.; Angelici, R. J. *Organometallics* **1989**, *8*, 14.

(11) Galperin, G. D. In *Chemistry of Heterocyclic Compounds*; Gronowitz, S. Ed.; Wiley: New York, 1986; Vol. 44, Part 2, p 355.

(12) Challenger, F. *Aspects of the Organic Chemistry of Sulfur*; Butterworths: London, 1959.

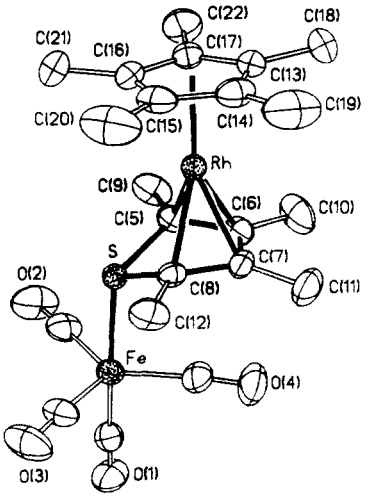

Figure 1. Structure of $Cp^*Rh\{(\eta^4:\eta^1\text{-}C_4Me_4S)Fe(CO)_4\}$ (2) with thermal ellipsoids drawn at the 35% probability level.

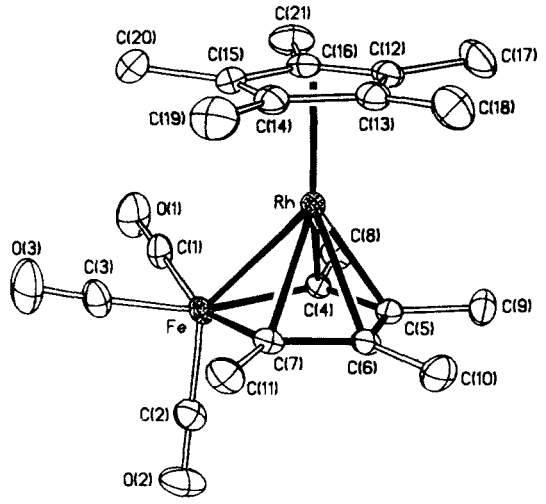

Figure 2. Structure of $Cp^*Rh\{\eta^5\text{-}C_4Me_4Fe(CO)_3\}$ (3) with thermal ellipsoids drawn at the 35% probability level.

carbon resonances is shifted upfield 70 ppm from $[1]^{2+}$. The symmetrical structure of compound **2** was also verified by X-ray crystallography. It consists of an $Fe(CO)_4$ unit bound to sulfur of the $Cp^*Rh(\eta^4\text{-}C_4Me_4S)$ "ligand" (Figure 1). The sulfur atom occupies an axial position on the trigonal-bipyramidal iron center. The Fe–S distance (2.303 (1) Å) is slightly longer than that of 2.288 (2) Å in (c-1,3-$C_4H_8S_2$)$Fe(CO)_4$,[13] possibly due to the existence of 2,5-methyl groups in C_4Me_4S. The average Fe–CO distance (1.782 (19) Å) is normal. The sufur atom of $\eta^4\text{-}C_4Me_4S$ lies out from the plane defined by C(1), C(2), C(3), and C(4). The sum of the angles about sulfur, C(5)–S–Fe (113.9 (1)°), C(8)–S–Fe (116.1 (1)°, and C(5)–S–C(8) (82.9 (2)°), clearly shows that the S atom is pyramidal. The average distance between Rh and C(5), C(6), and C(7) of C_4Me_4S, 2.109 (8) Å, is slightly shorter than the 2.140 (4) Å distance between Rh and C(8) of C_4Me_4S. Correspondingly, the C(7)–C(8) distance of 1.446 (6) Å is substantially longer than the other two C–C bonds (1.418 (6) and 1.407 (6) Å) in the C_4Me_4S ring. This difference is also observed in the closely related dimethylthiophene complex $Cp^*Ir(\eta^4\text{-}2,5\text{-}Me_2C_4H_2S\cdot BH_3)$.[9b] However, such variations in the C–C distances are not observed in $Fe(CO)_3\{(\eta^4:\eta^1\text{-}C_4H_4S)Re(CO)_2Cp^*\}$[14] and the sulfoxide $Cp^*Rh(\eta^4\text{-}C_4Me_4SO)$.[15]

Isolation and Structures of $Cp^*Rh\{\eta^5\text{-}C_4Me_4Fe(CO)_3\}$ (3) and $(Cp^*Rh)_2(\mu\text{-}CO)(\mu_3\text{-}S)Fe(CO)_3$ (4). Compound **2** reacts in refluxing toluene solutions to give two silica gel stable organometallic products. The first to elute is the yellow ferrole **3**, isolated in 53% yield as fluffy yellow crystals. When the thermolysis was conducted in the presence of 1 equiv of $Fe_3(CO)_{12}$, the yield of **3** was increased to ca. 65% and the second product was no longer observed. Solutions of **3** are stable under the reaction conditions; i.e., this cluster is unaffected by refluxing toluene in the presence or absence of C_4Me_4S. The ferrole exhibits a 5:2:2 pattern in its ^1H NMR spectrum consistent with a symmetric molecule; its IR spectrum features three strong bands in the ν_{CO} region.

The second product from the thermolysis of **2** is the red compound $(Cp^*Rh)_2FeS(CO)_4$ (**4**). Its yield also approaches 50% based on rhodium but diminishes greatly when the thermolysis is conducted in the presence of $Fe_3(CO)_{12}$. The formulation of **4** is based on the observation of a molecular ion in its field desorption mass spectrum and a single resonance in its ^1H NMR spectrum. The solution IR spectrum features three intense bands in the terminal ν_{CO} region and a weak broad band centered at 1750 cm^{-1}; the low-frequency band is more prominent for samples dispersed in KBr. The cluster **4** forms at the expense of **3**, since it contains two Cp*Rh and one $Fe(CO)_4$ fragments. It is partly for this reason that the addition of $Fe_3(CO)_{12}$ to the reaction mixture boosts the yield of **3**. The reaction solution from the thermolysis of **2** was also examined by gas chromatography. This showed that approximately half of the starting TMT in **2** is liberated in the course of the thermolysis.

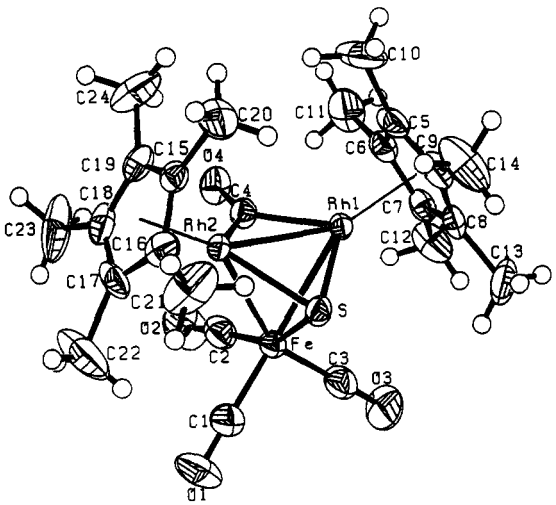

Figure 3. Structure of $(Cp^*Rh)_2(\mu\text{-}CO)(\mu_3\text{-}S)Fe(CO)_3$ (4) with thermal ellipsoids drawn at the 35% probability level.

Compound **3** is a sandwich complex. The Rh atom sits between two parallel and eclipsed planar rings (Figure 2). Its structure closely resembles that of the ferrarhodocene $CpRh\{\eta^5\text{-}C_4H_4Fe(CO)_3\}$[16] reported by McKennis et al. It is also related to $[1]^{2+}$, wherein S has been replaced by an $Fe(CO)_3$ unit. The planar heterocycle Fe–C(4)–C(5)–C(6)–C(7) is isostructural with the other ferroles.[17] The

(13) Cotton, F. A.; Stults, B. R. *Inorg. Chim. Acta* **1975**, *15*, 239.
(14) Choi, M.-G.; Angelici, R. J. *J. Am. Chem. Soc.* **1989**, *111*, 8755.
(15) Skaugset, A. E.; Rauchfuss, T. B.; Stern, C. A. *J. Am. Chem. Soc.* **1990**, *112*, 2432.

(16) $CpRh\{\eta^5\text{-}C_4H_4Fe(CO)_3\}$: King, M.; Holt, E. M.; Radnia, P.; McKennis, J. S. *Organometallics* **1982**, *1*, 1718.
(17) Listings of ferroles: (a) *Gmelin Handbuch der Anorganische Chemie*, 8th ed.; Springer-Verlag: Berlin, 1980; Part C3, pp 24–61. (b) Fehlhammer, W. P.; Stolzenberg, H. In *Comprehensive Organometallic Chemistry*; Wilkinson, G., Stone, F. G. A., Abel, E. W., Eds.; Pergamon Press: Oxford, U.K., 1982; Vol. 4, pp 548–555.

Table II. Mass Spectrometry Data for 3 and 3a from the Cothermolysis of 2 and 2a

	rel intens			
M$^+$, *m/e*	3 (obsd)[a]	3a (obsd)[a]	cothermolysis sample (obsd)[b]	random crossover (calcd)[b]
486	100	<0.01	100	100
488	4.65	<0.01	6.26	53.1
500	<0.01	7.40	16.14	100
502	<0.01	100	100	54.1

[a] Determined experimentally. [b] 2:1 molar ratio of 3 to 3a.

Fe–CO distance for the axial CO (Fe–C(2) = 1.769 (4) Å) is shorter than the other two Fe–CO distances (Fe–C(1) = 1.787 (4) Å, Fe–C(3) = 1.789 (4) Å, a phenomenon observed in all structurally characterized ferroles. The Fe–Rh distance 2.563 (1) Å is only slightly longer than 2.557 (2) Å in ferrarhodocene.[16] The bond lengths from Rh to the carbon atoms in the ferrole ring are slightly longer than those in 2.

Compound 4 features a tetrahedral Rh_2FeS core and can be described as (Cp*Rh)$_2$(μ-CO)(μ_3-S)Fe(CO)$_3$ (Figure 3). It is related to $Co_2FeS(CO)_9$.[6b] The iron center is approximately octahedral with a Rh_2–S–(CO)$_3$ coordination sphere. The Fe–Rh distances average 2.656 (12) Å. The rhodium centers are situated in a Cp*–Rh–(CO)–Fe–S coordination sphere with a Rh–Rh distance of 2.6811 (7) Å. The longest C–O distance is that of the bridging CO, as expected, while the remaining carbon–oxygen distances are typical of terminal CO ligands in iron carbonyls.

Double-Labeling Experiment. The mechanism of the thermolysis conversion of 2 to 3 was examined through a "double label" experiment, which probed the kinetic lability of the TMT–Rh bond. We first prepared and characterized (C_5Me_4Et)Rh{(η^4:η^1-C_4Me_4S-*3,4-d*$_2$)Fe(CO)$_4$} (**2a**). This compound was then thermolyzed in the presence of 2 equiv of unlabeled 2. The ferrole products were analyzed by electron impact mass spectrometry. Since the ratio of the ions at *m/e* 488/486 and 500/502 would be most sensitive to crossover, the relative intensities of these peaks are presented in Table II together with the values calculated for complete (random) crossover and the values measured for pure samples of 3 and **3a**. The experimental results indicate that the transformation of 2 to 3 occurs largely without formation of the crossover products (C_5Me_4Et)Rh{η^5-$C_4Me_4Fe(CO)_3$} (*m/e* 500 (M$^+$)) and Cp*Rh{η^5-$C_4Me_4Fe(CO)_3$-*3,4-d*$_2$} (*m/e* 488 (M$^+$)). On the basis of the *m/e* 488/486 ratio, crossover accounts for 3.3% of the ferrole product; the corresponding value is 4.9% on the basis of the *m/e* 500/502 ratio.

Discussion

Thermolysis of Cp*Rh{(η^4:η^1-C_4Me_4S)Fe(CO)$_4$}. The thermolysis of 1 proceeds approximately according to eq 4. All three organometallic compounds were characterized

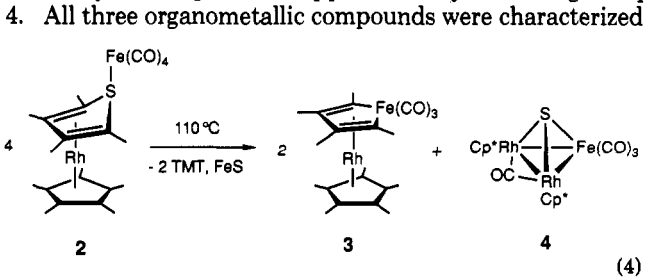

2 3 4 (4)

by single-crystal X-ray diffraction. On the basis of eq 4, the yield of 3, 4, and C_4Me_4S should each be 50%—we obtained 53, 46, and 59%, respectively. The efficacy of the conversion of 2 to 3 increases when the thermolysis of 2 is conducted in the presence of added $Fe_3(CO)_{12}$.

The labeling study shows that C_4Me_4S remains attached to the same rhodium center throughout the desulfurization. While we have no evidence concerning the kinetic stability of the S–Fe bond in 2, the double-labeling results allow us to rule out the following three desulfurization pathways.

(1) Species with the formula (Cp*Rh)$_2$(C_4Me_4S)[18] cannot be intermediates because they would give rise to exchange of the label. Such a species might have been expected in analogy to the thiaferroles $Fe_2SC_4R_4(CO)_6$, which are observed in the desulfurization of thiophenes by $Fe_3(CO)_{12}$.[5]

(2) The carbon skeleton of the thiophene does not rearrange in the course of the desulfurization since the deuterium label is not scrambled between the two types of methyl groups. This finding rules out cyclobutadiene intermediates such as Cp*Rh(η^4-C_4Me_4).[19]

(3) The thermolysis of 2 does not involve its fragmentation to give [Cp*RhS]$_x$ and $Fe_nC_4Me_4(CO)_m$, although both species (x = 4;[20] n = 2, m = 6[17]) have precedent.

The stoichiometry shown in eq 4 suggests that 2 binds an additional metal (Fe(CO)$_n$ or Cp*Rh) in the course of its desulfurization. The additional metals could serve as a sulfur acceptor while an iron atom replaces the sulfur in the heterocycle. Half of the 2 is consumed in the formation of 4; this gives rise to free TMT, the approximate stoichiometric amount of which was detected by gas chromatography. When the thermolysis was conducted in the presence of added $Fe_3(CO)_{12}$, 4 was formed only in trace amounts. We verified that 4 does not react with $Fe_3(CO)_{12}$ in refluxing toluene. This finding implies that the $Fe_3(CO)_{12}$ intercepts an intermediate that gives rise to 4.

This project began with the observation that 1 undergoes desulfurization upon treatment with $Fe_3(CO)_{12}$ to give 3. The tetracarbonyl 2 can be obtained in trace amounts from this reaction. Further evidence that 2 is an intermediate in the conversion 1 + $Fe_3(CO)_{12}$ → 3 is the finding that both the 1 + $Fe_3(CO)_{12}$ and the 2 + $Fe_3(CO)_{12}$ reactions give the same product 3 under very similar conditions (solvent, temperature, duration).

Relationship to Thiophene Desulfurization by Transition Metals. In the thermolysis 2, one set of metals combines to stabilize the hydrocarbon residue in the form of a ferrole, while a second group of metals binds the extruded sulfur atom to give a cluster. Thus, the metals play two distinct roles in the desulfurization of the heterocycle. The initial stage in thiophene desulfurization constitutes the replacement of one heteroatom with another, i.e. metal for sulfur. The metallacyclic ferrole provides an obvious means for the stabilization of the hydrocarbon residue. With regard to subsequent steps in a hydrodesulfurization cycle, the formation of M–C bonds is necessary simply because they are susceptible to hydrogenolysis, whereas C–S bonds are not (eq 5).

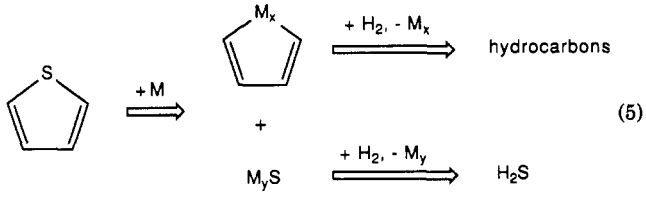

(5)

(18) Luo, S.; Ogilvy, A. E.; Rauchfuss, T. B.; Rheingold, A. L.; Wilson, S. R. Unpublished results.

(19) CpRh(C_4H_4) and CpRh(C_4Ph_4): Gardner, S. A.; Rausch, M. D. *J. Organomet. Chem.* **1973**, *56*, 365. Cash, G. G.; Helling, J. F.; Mathew, M.; Palenik, G. J. *J. Organomet. Chem.* **1973**, *50*, 277.

(20) Skaugset, A. E.; Rauchfuss, T. B.; Wilson, S. R. *Organometallics* **1990**, *9*, 2875.

The desulfurization of **2** is noteworthy because the fates of both the hydrocarbon and extruded sulfide are well-defined. Previous work on thiophene desulfurization by organometallic reagents had demonstrated *either* the formation of sulfido clusters *or* the formation of metallacycles. Surface science studies of thiophene HDS on Mo(100) showed that sulfur initially binds at "four-fold hollow sites".[3g] This environment provides the sulfur atom with a high coordination number. The formation of **4** with a triply bridging sulfido group provides comparable stabilization. The structural similarity between **3** and $[1]^{2+}$ is striking. The coordination number of the sulfur atom in **4** is the same as that in $[1]^{2+}$, i.e. the desulfurization of η^5-C_4Me_4S entails replacement of two C–S bonds by two M–S bonds.

In the homogeneous reaction **2** → **3** + **4** (eq 4), the desulfurization of 1 equiv of thiophene requires the action of *five* metals. This aspect demonstrates the advantages of multimetallic desulfurization agents such as clusters and surfaces. The finding that both the hydrocarbon and sulfur are stabilized in heterometallic enviroinments is reminiscent of the synergism well-known for bimetallic hydrodesulfurization catalysts.[21]

Experimental Section

Rhodium trichloride hydrate was obtained from Johnson Matthey, Inc. $[Cp^*RhCl_2]_2$ was prepared by the reaction of rhodium trichloride with either hexamethyl Dewar benzene or with pentamethylcyclopentadiene.[22] $[(C_5Me_4Et)RhCl_2]_2$ was prepared by the similar reaction of ethanolic rhodium trichloride with ethyltetramethylcyclopentadiene (Aldrich).[23] 2,5-Dimethylthiophene (Penta Chemical Co.) was distilled from $MgSO_4$ at 1 atm. Silver trifluoromethanesulfonate (Aldrich) and $Fe(CO)_5$ (Aldrich) were used as received. Me_3NO (Aldrich) was sublimed before use. $Fe_3(CO)_{12}$ was prepared according to the literature method.[24] Cp_2Co was prepared from NaCp and $CoCl_2$ and sublimed before use. Acetone was reagent grade and was purged with nitrogen for about 1 h before use. Hexane was distilled from CaH_2. Toluene was distilled from sodium. All manipulations were carried out under a nitrogen atmosphere with use of standard Schlenk techniques.

^1H NMR spectra (chemical shifts vs internal tetramethylsilane) were recorded on Varian XL 200 (200 MHz) and General Electric QE 300 (300 MHz) spectrometers. ^{13}C NMR spectra were collected on the QE 300 instrument (75 MHz) as well as a General Electric GN 500 (125 MHz) spectrometer. The HETCOR NMR experiment was conducted on the GN 500 spectrometer. FD (field desorption) and 70-eV EI (electron impact) mass spectral analyses were carried out by the University of Illinois Mass Spectrometry Laboratory. Elemental analyses were performed by the University of Illinois Microanalytical Laboratory. Infrared spectra were recorded on a Perkin-Elmer 1750 Fourier transform spectrometer. GC analyses were carried out on a Hewlett-Packard 5890 gas chromatograph with a Spectra-Physics 3390A integrator and an HP-1 silicone gum column (10 m × 0.53 mm × 2.65 μm).

3,4-Bis(chloromethyl)-2,5-dimethylthiophene. This procedure was adapted from that described originally by Dimroth et al.[25] A solution of *s*-trioxane (38.9 g, 1.32 mol) in glacial acetic acid (170 mL) was prepared in a 500-mL three-neck round-bottom flask equipped with a gas inlet attached to a cylinder of HCl gas. The solutioin was saturated with the HCl. While the HCl gas flow was maintained, 2,5-dimethylthiophene (37.0 g, 0.32 mol) was added dropwise at 0 °C. During the addition, the initially colorless solution became pale red and finally red-brown. The addition requires ca. 1 h. Stirring was continued at 0 °C for another 1 h, resulting in the formation of a large amount of white precipitate. The ice bath was then removed from the bluish slurry. If, at this stage, the reaction mixture began to spontaneously warm, it was again cooled with the ice bath. The reaction temperature should not exceed 65 °C. This warming and cooling cycle was repeated (with continuous HCl gas flow) until no reaction was evident at room temperature. The mixture was then cooled to 0 °C for 1 h and filtered in air with use of a medium-porosity frit. The pale yellow product was washed with glacial acetic acid (ca. 20 mL), leaving an almost colorless solid, which was vacuum-dried; yield 50.02 g (72.5%, based on 2,5-dimethylthiophene). Additional impure product can sometimes be obtained by diluting the acetic acid filtrate with water. ^1H NMR ($CDCl_3$): δ 4.60 (s, 4 H), 2.40 (s, 6 H).

Tetramethylthiophene. This procedure is adapted from that first reported by Tonkyn et al.[26] A 1000-mL, three-necked flask is equipped with a reflux condenser a mechanical stirrer, a Y-shaped connector that is attached to a N_2 inlet, and an equal-pressure addition funnel. After it is purged with N_2, 300 mL of freshly distilled THF is added to the flask by syringe. At 0 °C, solid $LiAlH_4$ (15.0 g, 0.40 mol) is added to the flask with continuous N_2 flow and vigorous stirring. (This addition can be very exothermic.) After the addition, the slurry thus obtained is cooled to 0 °C. In another 500-mL flask, 3,4-bis(chloromethyl)-2,5-dimethylthiophene (31.8 g, 0.15 mol) is dissolved in 400 mL of THF. This solution is transferred to the addition funnel through a cannula followed by washing the flask with a 10-mL portion of THF. This solution is added dropwise to the above $LiAlH_4$/THF slurry at 0 °C. The exothermic reaction occurs immediately. During the addition process the reaction mixture is maintained at 0 °C. The addition should take ca. 2–3 h. After it is stirred at 0 °C for a further 1 h, the slurry is heated to reflux overnight. The excess $LiAlH_4$ is destroyed by adding solid $Na_2SO_4 \cdot 10H_2O$ to the cooled (0 °C) reaction mixture under a flow of N_2. After all of the $LiAlH_4$ is destroyed (a few drops of water is used to test for completeness), the slurry is filtered in air through Celite. The solid residue left in the filter is transferred to a 1000-mL flask and thoroughly extracted with 600 mL of refluxing diethyl ether. The extracts are combined and concentrated in vacuo. The light yellow liquid thus obtained is distilled under 1 atm. The clear distillate (180–185 °C) is collected; yield 15.7 g (73.7%, based on 3,4-bis(chloromethyl)-2,5-dimethylthiophene). ^1H NMR ($CDCl_3$): δ 2.00 (6 H), 2.30 (6 H).

Preparation of $[Cp^*Rh(\eta^5\text{-}C_4Me_4S)](OTf)_2$ ([1](OTf)$_2$) and $[(C_5Me_4Et)Rh(\eta^5\text{-}C_4Me_4S\text{-}3,4\text{-}d_2)](OTf)_2$ ([1a](OTf)$_2$). The following procedure was adapted from Maitlis and co-workers.[27] An acetone solution (20 mL) of AgOTf (1.88 g, 7.30 mmol) was added in one portion to an acetone suspension (30 mL) of $[Cp^*RhCl_2]_2$ (1.12 g, 1.81 mmol) and TMT (0.9 mL, 6.42 mmol). The homogeneous red solution immediately turned yellow with concomitant precipitation of AgCl. After 2 h, the solution was filtered through Celite in air. The yellow filtrate was concentrated to ca. 10 mL. Pale yellow crystals of $[Cp^*Rh(\eta^5\text{-}C_4Me_4S)](OTf)_2$ were obtained by slow addition of $CHCl_3$ to the concentrated filtrate; yield 2.09 g (86%, based on $[Cp^*RhCl_2]_2$). ^1H NMR (CD_3COCD_3): δ 2.64 (s, 6 H), 2.43 (s, 6 H), 2.24 (s, 15 H). ^{13}C NMR (CD_3COCD_3, $J(^{103}Rh,^{13}C)$ in Hz): δ 122.07 (C_4Me_4), 121.07 (OSO_2CF_3, $J(^{19}F, ^{13}C)$ = 322) 118.30 (C_4Me_4, 6.8) 110.71 (C_5Me_5, 8.1) 12.56 (C_5Me_5), 10.97 (C_4Me_4), 9.68 (C_4Me_4). Anal. Calcd for $C_{20}H_{27}F_6O_6RhS_3$: C, 35.49; H, 4.02; S, 14.22. Found: C, 35.51; H, 4.07; S, 14.34. $[(C_5Me_4Et)Rh(\eta^5\text{-}C_4Me_4S\text{-}3,4\text{-}d_2)](OTf)_2$ was prepared in the same way by starting from $[(C_5Me_4Et)RhCl_2]_2$ and $C_4Me_4S\text{-}3,4\text{-}d_2$. ^1H NMR (CD_3COCD_3): δ 2.67 (quart, CH_2CH_3), 2.66 (s, 6 H, 2,5-CH_3 of TMT-3,4-d_2), 2.43 (1:1:1 t, 3,4-CH_2D of TMT), 2.29 (s, 6 H), 2.28 (s, 6 H), 1.22 (t, CH_2CH_3).

Preparation of $Cp^*Rh(\eta^4\text{-}C_4Me_4S)$ (1) and $(C_5Me_4Et)Rh(\eta^4\text{-}C_4Me_4S\text{-}3,4\text{-}d_2)$ (1a). A yellow acetone suspension (20 mL) of [1](OTf)$_2$ (1.037 g, 1.533 mmol) was cooled to −78 °C. To this was added a red-brown solution of Cp_2Co (0.608 g, 3.215 mmol) in acetone (15 mL) in small portions via cannula. The addition requires ca. 0.5 h. The dark red reaction mixture was warmed slowly to room temperature. After it was concentrated to half of its original volume, the solution was diluted with an equal

(21) Harris, S.; Chianelli, R. R. *J. Catal.* **1986**, *98*, 17.
(22) Kang, J. W.; Moseley, K.; Maitlis, P. M. *J. Am. Chem. Soc.* **1969**, *91*, 5970.
(23) Dooley, T.; Fairhurst, G.; Chalk, C. D.; Tabatabaian, K.; White, C. *Transition Met. Chem.* **1978**, *3*, 299.
(24) King, R. B.; Stone, F. G. A. *Inorg. Synth.* **1963**, *7*, 193.
(25) Dimroth, K.; Pohl, G.; Follmann, H. *Chem. Ber.* **1966**, *99*, 634.
(26) Gaertner, R.; Tonkyn, R. G. *J. Am. Chem. Soc.* **1951**, *73*, 5872.
(27) Russell, M. J. H.; White, C.; Yates, A.; Maitlis, P. M. *J. Chem. Soc., Dalton Trans.* **1978**, 857.

volume of hexane and filtered to remove a yellow solid consisting primarily of $[Cp_2Co][CF_3SO_3]$. The cycle of hexane addition followed by concentration in vacuo was repeated until no more yellow solid was observed. The resulting dark red solution was then evaporated to give red microcrystalline Cp*Rh(η^4-C_4Me_4S), yield 0.546 g (94%, based on Rh). ^{1}H NMR (CD_3COCD_3): δ 1.98 (s, 6 H), 1.71 (s, 15 H), 1.13 (s, 6 H). ^{13}C NMR (CD_3COCD_3, $J(^{103}Rh,^{13}C)$ in Hz): δ 94.58 (C_5Me_5, 6.2), 88.43 (C_4Me_4, 7.3), 42.87 (C_4Me_4, 14.8), 15.25 (C_4Me_4), 11.31 (C_4Me_4), 9.50 (C_5Me_5). EIMS (70 eV): m/e 378 (65%, M^+), 238 (100%, $M^+ - C_8H_{12}S$). Anal. Calcd for $C_{18}H_{27}RhS$: C, 57.24; H, 7.19; S, 8.47. Found: C, 57.33; H, 7.27; S, 8.20. Similarly, (C_5Me_4Et)Rh(η^4-C_4Me_4S-*3,4-d*$_2$) was prepared by the Cp_2Co reduction of [(C_5Me_4Et)Rh(η^5-C_4Me_4S-*3,4-d*$_2$)]$(OTf)_2$. ^{1}H NMR (C_6D_6): δ 2.07 (quart, CH_2CH_3), 1.79 (1:1:1 t, 3,4-CH_2D of TMT), 1.66 (s, 6 H), 1.64 (s, 6 H), 1.19 (s, 2,5-CH_3 of TMT), 1.05 (t, CH_2CH_3).

Preparation of Cp*Rh{(η^4:η^1-C_4Me_4S)Fe(CO)$_4$} (2) and (C_5Me_4Et)Rh{(η^4:η^1-C_4Me_4S-*3,4-d*$_2$)Fe(CO)$_4$} (2a). A red acetone solution (20 mL) of Cp*Rh(η^4-C_4Me_4S) (778 mg, 2.02 mmol) in a 100-mL Schlenk flask was frozen in liquid nitrogen. To this frozen mass was added a suspension of Me_3NO (170 mg, 2.20 mmol) in acetone (20 mL) followed by $Fe(CO)_5$ (280 μL, 2.14 mmol). The frozen mixture was warmed to room temperature and stirred for 2 h. The reddish yellow solution was then filtered through Celite and concentrated to 10 mL to give yellow microcrystals of Cp*Rh{(η^4:η^1-C_4Me_4S)Fe(CO)$_4$}, which were collected by filtration. More product was obtained upon further concentration of the filtrate; combined yield 850 mg (76%, based on Rh). ^{1}H NMR (C_6D_6): δ 1.57 (s, 6 H), 1.30 (s, 15 H), 1.23 (s, 6 H). ^{13}C NMR (C_6D_6, $J(^{103}Rh,^{13}C)$ in Hz): δ 216.51 (*C*O), 94.79 (C_5Me_5, 6.3), 90.26 (C_4Me_4, 6.6), 52.74 (C_4Me_4, 15.3), 12.33 (C_4Me_4), 10.69 (C_4Me_4), 9.00 (C_5Me_5). FDMS: m/e 546 (M^+ for ^{56}Fe) 486 ($M^+ - COS$, 378 ($M^+ - Fe(CO)_4$). IR (hexane, cm^{-1}): ν_{CO} = 2034 (s) 1959 (m), 1933 (s), 1923 (s). Anal. Calcd for $C_{22}H_{27}FeO_4RhS$: C, 48.37; H, 4.98; S, 5.87. Found: C, 48.31; H, 5.05; S, 5.83. The crystal for X-ray diffraction experiment was obtained by cooling a concentrated hexane solution. (C_5Me_4Et)Rh{(η^4:η^1-C_4Me_4S-*3,4-d*$_2$)Fe(CO)$_4$} was prepared from (C_5Me_4Et)Rh(η^4-C_4Me_4S-*3,4-d*$_2$) in a similar way. ^{1}H NMR (C_6D_6): δ 1.72 (quart, CH_2CH_3), 1.57 (1:1:1 t, 3,4-CH_2D of TMT), 1.32 (s, 6 H), 1.29 (s, 6 H), 1.24 (s, 2,5-CH_3 of TMT), 0.81 (t, CH_2CH_3).

Thermolysis of Cp*Rh(η^4-C_4Me_4S) in the Presence of $Fe_3(CO)_{12}$. A mixture of $Fe_3(CO)_{12}$ (180 mg, 0.36 mmol) and Cp*Rh(η^4-C_4Me_4S) (120 mg, 0.32 mmol) in toluene (30 mL) was heated at reflux for 18 h to give a dark yellow solution with a mirrorlike deposit on the sides of the flask. The cooled reaction mixture was filtered through Celite in air. The yellow filtrate was evaporated and flash-chromatographed on silica gel with 2:1 hexane/CH_2Cl_2 as eluent to give analytically pure Cp*Rh{η^5-$C_4Me_4Fe(CO)_3$} after solvent removal; yield 58 mg (37%, based on Rh). ^{1}H NMR (C_6D_6): δ 2.29 (s, 6 H), 1.43 (s, 15 H), 1.31 (s, 6 H). ^{13}C NMR (CD_3COCD_3, $J(^{103}Rh,^{13}C)$ in Hz): δ 215.74 (*C*O), 167.64 (C_4Me_4, 18.3), 113.16 (C_4Me_4), 97.13 (C_5Me_5, 7.3), 28.50 (C_4Me_4), 12.30 (C_4Me_4), 9.80 (C_5Me_5). IR (hexane, cm^{-1}): ν_{CO} = 1994, 1939, and 1935 (sh). FDMS: m/e 486 (M^+ for ^{56}Fe). Anal. Calcd for $C_{21}H_{27}FeO_3Rh$: C, 51.85; H, 5.60. Found: C, 51.85; H, 5.64.

Thermolysis of Cp*Rh{(η^4:η^1-C_4Me_4S)Fe(CO)$_4$}. Isolation of (Cp*Rh)$_2$(μ-CO)(μ_3-S)Fe(CO)$_3$ (4). A solution of Cp*Rh{(η^4:η^1-C_4Me_4S)Fe(CO)$_4$} (100 mg, 0.184 mmol) in toluene (15 mL) was heated to reflux for ca. 60 h. The cooled reaction solution was filtered through Celite to remove the black residue. The filtrate was concentrated under vacuum and loaded onto a 2 × 30 cm column of silica gel. Elution with 2:1 hexane/CH_2Cl_2 gave a faster first yellow band followed by a red band. The first fraction afforded an intensely yellow fluffy solid whose ^{1}H NMR spectrum matched that for Cp*Rh{η^5-$C_4Me_4Fe(CO)_3$}, yield 48.0 mg (53.6%, based on Rh). Evaporation of the second fraction gave **4** as dark red microcrystals, yield 28.7 mg (46.1% based on Rh). ^{1}H NMR (C_6D_6): δ 1.71 (s). FDMS: m/e 676 (M^+ for ^{56}Fe). IR (KBr, cm^{-1}): ν_{CO} = 1997, 1928, 1752. The crystal for X-ray diffraction was grown by cooling a concentrated hexane solution. In a separate thermolysis experiment, 100 mg of **2** yielded 15 mg of TMT (59%, based on **2**) on the basis of gas chromatographic analysis.

Thermolysis of Cp*Rh{(η^4:η^1-C_4Me_4S)Fe(CO)$_4$} in the Presence of $Fe_3(CO)_{12}$. Cp*Rh{(η^4:η^1-C_4Me_4S)Fe(CO)$_4$} (50.7 mg, 0.0928 mmol) and $Fe_3(CO)_{12}$ (46.5 mg, 0.0923 mmol) was dissolved in toluene (15 mL). The greenish solution was heated to reflux for ca. 20 h. After it was cooled, the reddish yellow solution was filtered to remove the black residue. The filtrate was concentrated and subjected to silica gel chromatography. Elution with 2:1 hexane/CH_2Cl_2 gave a yellow band followed by a red band, which decomposed on the column. The first fraction yielded a bright yellow fluffy solid after vacuum removal of the solvents; yield 28.7 mg (64% based on Rh). The ^{1}H NMR spectrum was identical with that for Cp*Rh{η^5-$C_4Me_4Fe(CO)_3$}.

Thermolysis of (C_5Me_4Et)Rh{(η^4:η^1-C_4Me_4S-*3,4-d*$_2$)Fe(CO)$_4$} in the Presence of $Fe_3(CO)_{12}$. A toluene solution (10 mL) of (C_5Me_4Et)Rh{(η^4:η^1-C_4Me_4S-*3,4-d*$_2$)Fe(CO)$_4$} (50.0 mg, 0.0889 mmol) and $Fe_3(CO)_{12}$ (44.8 mg, 0.0889 mmol) in a 100-mL Schlenk flask was heated to reflux for 20 h. After it was cooled, the solution was filtered and concentrated. The resulting reddish yellow solution was loaded onto a silica gel column and eluted with 2:1 hexane/CH_2Cl_2. Evaporation of the fast-moving yellow band gave 12 mg (27%, based on Rh) of (C_5Me_4Et)Rh{(η^5-$C_4Me_4Fe(CO)_3$-*3,4-d*$_2$}. ^{1}H NMR (C_6D_6): δ 2.25 (s, 6 H), 1.90 (quart, CH_2CH_3), 1.43 (s, 6 H), 1.38 (s, 6 H), 1.27 (1:1:1 t, 3,4-CH_2D of TMT), 0.69 (t, CH_2CH_3). FDMS: m/e 502 (M^+ for ^{56}Fe).

Cothermolysis of Cp*Rh{(η^4:η^1-C_4Me_4S)Fe(CO)$_4$} and (C_5Me_4Et)Rh{(η^4:η^1-C_4Me_4S-*3,4-d*$_2$)Fe(CO)$_4$}. A toluene solution (10 mL) of Cp*Rh{(η^4:η^1-C_4Me_4S)Fe(CO)$_4$} (56.0 mg, 0.112 mmol) and (C_5Me_4Et)Rh{(η^4:η^1-C_4Me_4S-*3,4-d*$_2$)Fe(CO)$_4$} (28.0 mg, 0.0557 mmol) was heated at reflux for 24 h. After it was cooled, the solution was directly loaded on a silica gel column. Elution of the yellow band with 2:1 hexane/CH_2Cl_2 followed by evaporation gave 28 mg of yellow microcrystals (34%, based on Rh). EIMS (70 eV) showed two molecular ion envelopes centered at m/e 486 and 502.

The percent crossover was calculated for both the m/e 488/486 and 502/500 ratios. Shown below is the calculation for the m/e 488/486 ratio, where I_x is the intensity of an ion at $m/e = x$:

$$\text{range of isotope effect} = R = [I_{488}/I_{486}]_{\text{random}} - [I_{488}/I_{486}]_3 = 48.45$$

$$\%\ \text{crossover} = 100([I_{488}/I_{486}]_{\text{exp}} - [I_{488}/I_{486}]_3)/R$$

Thermolysis of (Cp*Rh)$_2$(μ-CO)(μ_3-S)Fe(CO)$_3$ in the Presence of $Fe_3(CO)_{12}$. (Cp*Rh)$_2$(μ-CO)(μ_3-S)Fe(CO)$_3$ (12.1 mg, 0.0178 mmol) and $Fe_3(CO)_{12}$ (10.1 mg, 0.020 mmol) were dissolved in 5 mL of toluene. The solution was heated to reflux for 20 h. After it was cooled, the solution was filtered, leaving a black solid and iron film. Thin-layer chromatography of the filtrate on silica gel plates (developed with 2:1 hexane/CH_2Cl_2) showed the same R_f value as that of the pure **4**.

X-ray Analysis: Cp*Rh{(η^4:η^1-C_4Me_4S)Fe(CO)$_4$}. The red crystal was mounted on a glass fiber with epoxy cement. Unit cell parameters were obtained from the least-squares fit of 25 reflections ($20° \le 2\theta \le 25°$). Preliminary photographic characterization showed $2/m$ Laue symmetry. Systematic absences in the diffraction data uniquely established the space group as $P2_1/n$. No absorption correction was applied to the data set (low μ, well-shaped crystal, T_{max}/T_{min} = 1.012). The structure was solved by direct methods, which located the Fe and Rh atoms. The remaining non-hydrogen atoms were located from subsequent Fourier synthesis. All non-hydrogen atoms were refined with anisotropic thermal parameters. Hydrogen atoms were included as idealized isotropic contributions (d(CH) = 0.960 Å, U = 1.2 Å^2 for attached C). Crystal, data collection, and refinement parameters are listed in Table III. Atomic coordinates and isotropoic thermal parameters are listed in Table IV. Selected bond distances and angles are listed in Table V.

Cp*Rh{η^5-$C_4Me_4Fe(CO)_3$}. A yellow crystal was mounted on a glass fiber with epoxy cement. Systematic absences and diffraction symmetry initially suggested either the hexagonal space group $P63$ or $P63/m$. However, accurate determination of the unit-cell metrics with use of high-angle data gave γ = 119.336 (11)°; TRACER (DEL = 0.1) established orthorhombic symmetry. Photographic characterization of the unit cell confirmed *mmm* Laue symmetry. Systematic absences in the diffraction data suggested either $Pnma$ or $pn2_1a$. The acentric alternative was suggested by E statistics and was confirmed by the chemically sensible refinement. No absorption correction was required (low

Table III. X-ray Crystallographic Data for Cp*Rh{(η^4:η^1-C_4Me_4S)Fe(CO)$_4$} (2), Cp*Rh{η^5-$C_4Me_4Fe(CO)_3$} (3), and (Cp*Rh)$_2$(μ-CO)(μ_3-S)Fe(CO)$_3$ (4)

	2	3	4
formula	$C_{22}H_{22}FeO_4RhS$	$C_{21}H_{27}FeO_3Rh$	$C_{24}H_{30}FeO_4Rh_2S$
cryst syst	monoclinic	orthorhombic	monoclinic
space group	$P2_1/n$	$Pn2_1a$	$P2_1/n$
a, Å	9.8747 (23)	14.9366 (26)	11.933 (2)
b, Å	16.401 (3)	15.6529 (18)	14.699 (3)
c, Å	14.983 (3)	8.7393 (10)	15.157 (3)
β, deg	96.849 (20)	90	99.34 (1)
V, Å^3	2409.3 (9)	2043.3 (5)	2636 (2)
Z	4	4	4
ρ_{calcd}, g cm^{-3}	1.492	1.581	1.704
color	dark red	yellow	black
T, K	296	296	299
μ(Mo Kα), cm^{-1}	13.76	15.06	18.64
diffractometer	Nicolet R3m	Nicolet R3m	Syntex $P2_1$
radiation		Mo Kα (λ = 0.17073 Å)	
monochromator		graphite	
scan type	Wyckoff	Wyckoff	$\omega/2\theta$
scan speed, deg min^{-1}	variable, 7–20	variable, 6–20	6
scan range, deg	$4 \le 2\theta \le 52$	$4 \le 2\theta \le 55$	$3 \le 2\theta \le 46$
no. of rflns collected	5107	5247	4183
no. of indpt rflns	4736	4771	3365
no. of indpt rflns obsd	3676[a]	4142[a]	2905[b]
std rflns	3 std/197 rflns	3 std/197 rflns	3 std/100 rflns
$R(F)$, %	3.57	2.45	3.2
$R(wF)$, %	3.91	2.54	4.2
$\Delta(\rho)$, e Å^{-3}	0.579	0.565	0.60
GOF	1.041	1.009	

[a] $F_o > 5\sigma(F_o)$. [b] $I > 2.85\sigma(I)$.

Table IV. Atomic Coordinates (×10^4) and Isotropic Thermal Parameters (Å^2 × 10^3) for Cp*Rh{(η^4:η^1-C_4Me_4S)Fe(CO)$_4$}

atom	x	y	z	U[a]
Rh	3751.3 (3)	5747.9 (2)	2127.7 (2)	35.5 (1)
Fe	6155.8 (6)	8104.4 (4)	942.1 (4)	46.4 (2)
S	5173 (1)	6851 (1)	1108 (1)	39 (1)
O(1)	7099 (5)	9769 (2)	707 (3)	93 (2)
O(2)	4317 (5)	8238 (3)	−739 (3)	114 (2)
O(3)	8779 (4)	7340 (3)	728 (3)	104 (2)
O(4)	5742 (5)	8566 (2)	2780 (3)	104 (2)
C(1)	6750 (5)	9107 (3)	794 (3)	62 (2)
C(2)	5007 (5)	8180 (3)	−77 (4)	70 (2)
C(3)	7739 (5)	7622 (3)	806 (4)	64 (2)
C(4)	5868 (6)	8367 (3)	2067 (3)	67 (2)
C(5)	3540 (4)	6904 (2)	1498 (3)	45 (1)
C(6)	3657 (4)	6997 (2)	2448 (3)	51 (1)
C(7)	4930 (4)	6674 (2)	2841 (2)	45 (1)
C(8)	5674 (4)	6357 (2)	2157 (2)	41 (1)
C(9)	2366 (4)	7204 (3)	833 (4)	74 (2)
C(10)	2625 (6)	7407 (3)	2956 (4)	88 (2)
C(11)	5439 (6)	6669 (3)	3826 (3)	80 (2)
C(12)	7084 (4)	5998 (3)	2306 (3)	63 (2)
C(13)	2254 (5)	4937 (3)	2711 (3)	55 (2)
C(14)	3549 (5)	4591 (3)	2880 (3)	61 (2)
C(15)	4015 (4)	4425 (3)	2034 (4)	61 (2)
C(16)	2983 (4)	4683 (3)	1335 (3)	54 (2)
C(17)	1919 (4)	5012 (3)	1764 (3)	51 (1)
C(18)	1341 (6)	5193 (4)	3396 (4)	93 (3)
C(19)	4287 (7)	4378 (4)	3789 (4)	115 (3)
C(20)	5298 (6)	3999 (3)	1891 (5)	111 (3)
C(21)	3008 (7)	4572 (4)	346 (4)	96 (3)
C(22)	578 (5)	5317 (4)	1284 (4)	84 (2)

[a] Equivalent isotropic U defined as one-third of the trace of the orthogonalized U_{ij} tensor.

Table V. Selected Bond Distances and Angles for Cp*Rh{(η^4:η^1-C_4Me_4S)Fe(CO)$_4$}

Bond Distances (Å)			
Rh–S	2.871 (1)	Rh–C(5)	2.114 (4)
Rh–C(6)	2.110 (4)	Rh–C(7)	2.103 (4)
Rh–C(8)	2.140 (4)	Fe–S	2.303 (1)
S–C(5)	1.800 (4)	S–C(8)	1.771 (4)
C(5)–C(6)	1.418 (6)	C(6)–C(7)	1.407 (6)
C(7)–C(8)	1.446 (6)	Fe–C(1)	1.772 (5)
Fe–C(2)	1.761 (5)	Fe–C(3)	1.792 (5)
Rh–CNT[a]	1.852 (4)	Fe–C(4)	1.804 (5)
Bond Angles (deg)			
Rh–S–Fe	150.3 (1)	CNT–Rh–C(8)	143.4 (2)
CNT–Rh–C(5)	143.3 (2)	CNT–Rh–S	145.3 (1)
CNT–Rh–C(7)	148.2 (2)	C(5)–Rh–C(8)	67.5 (1)
C(5)–Rh–C(6)	39.2 (2)	C(6)–Rh–C(7)	39.0 (2)
C(5)–Rh–C(7)	65.6 (1)	C(7)–Rh–C(8)	39.8 (2)
C(6)–Rh–C(8)	67.2 (2)	C(5)–S–C(8)	82.9 (2)
Fe–S–C(5)	113.9 (1)	S–C(5)–C(6)	113.1 (3)
Fe–S–C(8)	116.1 (1)	S–C(5)–C(9)	116.2 (3)
Rh–C(6)–C(5)	70.6 (2)	C(5)–C(6)–C(7)	108.0 (4)
Rh–C(6)–C(7)	70.2 (2)	Rh–C(7)–C(6)	70.7 (2)
Rh–C(6)–C(10)	126.9 (3)	C(6)–C(7)–C(8)	111.0 (3)
Rh–C(7)–C(8)	71.5 (2)	Rh–C(8)–S	94.0 (1)
Rh–C(7)–C(11)	125.3 (3)	S–C(8)–C(7)	111.2 (3)
Rh–C(8)–C(7)	68.7 (2)	S–C(8)–C(12)	116.6 (3)
Rh–C(8)–C(12)	128.5 (3)	S–Fe–C(1)	174.5 (2)
CNT–Rh–C(6)	147.0 (2)	S–Fe–C(2)	86.0 (2)
C(1)–Fe–C(2)	90.5 (2)	S–Fe–C(3)	90.4 (2)
C(1)–Fe–C(3)	94.8 (2)	S–Fe–C(4)	89.0 (2)
C(1)–Fe–C(4)	89.9 (2)	C(3)–Fe–C(4)	118.5 (2)
C(2)–Fe–C(3)	112.9 (2)	C(2)–Fe–C(4)	128.3 (2)

[a] CNT is the centroid of atoms C(13) to C(17).

μ, well-shaped crystal, T_{max}/T_{min} = 1.06). The structure was solved by direct methods. The remaining non-hydrogen atoms were located from subsequent difference Fourier syntheses. The hydrogen atoms were included in the refinement as a mix of found and idealized (d(CH) = 0.960 Å, U = 1.2U for attached C) isotropic contributions to obtain their correct rotational orientations. All non-hydrogen atoms were refined with anisotropic thermal parameters. Refinement of a multiplication term for $\Delta f''$ produced a value of 1.03 (3), indicating the correctness of the enantiomorph reported. Crystal, data collection, and refinement parameters are listed in Table III. Atomic coordinates and isotropic thermal parameters are listed in Table VI. Selected bond distances and angles are listed in Table VII.

(Cp*Rh)$_2$(μ-CO)(μ_3-S)Fe(CO)$_3$. The dark, opaque, equidimensional crystal was mounted with use of epoxy to a thin glass fiber. Final cell dimensions were obtained from the least-squares fit of 15 reflections ($9.6° \le 2\theta \le 19.9°$). The space group $P2_1/n$ was unambiguously determined from the systematic absences.

Table VI. Atomic Coordinates (×10^4) and Isotropic Thermal Parameters (Å^2 × 10^3) for Cp*Rh{η^5-C_4Me_4Fe(CO)$_3$}

atom	*x*	*y*	*z*	*U*[a]
Rh	6897.0 (1)	7500	−51.2 (2)	23.2 (1)
Fe	7910.9 (3)	6199.3 (4)	−460.9 (5)	28.0 (1)
O(1)	7509 (2)	5584 (2)	−3541 (3)	70 (1)
O(2)	9733 (2)	5582 (3)	−8 (3)	70 (1)
O(3)	6882 (2)	4754 (2)	737 (4)	77 (1)
C(1)	7678 (2)	5830 (2)	−2354 (4)	41 (1)
C(2)	9021 (3)	5832 (3)	−205 (4)	42 (1)
C(3)	7303 (3)	5310 (2)	298 (4)	43 (1)
C(4)	8152 (2)	7360 (2)	−1237 (3)	27 (1)
C(5)	8264 (2)	7998 (2)	−101 (3)	30 (1)
C(6)	8054 (2)	7714 (2)	1416 (4)	30 (1)
C(7)	7796 (2)	6836 (2)	1479 (4)	31 (1)
C(8)	8318 (2)	7593 (3)	−2892 (4)	40 (1)
C(9)	8554 (2)	8911 (2)	−433 (4)	45 (1)
C(10)	8092 (2)	8286 (3)	2786 (4)	46 (1)
C(11)	7570 (2)	6451 (2)	3000 (4)	43 (1)
C(12)	5900 (2)	8447 (2)	−855 (4)	37 (1)
C(13)	5724 (2)	8249 (2)	723 (4)	37 (1)
C(14)	5522 (2)	7359 (2)	815 (4)	36 (1)
C(15)	5578 (2)	7004 (2)	−688 (4)	38 (1)
C(16)	5817 (2)	7686 (2)	−1718 (4)	37 (1)
C(17)	6087 (3)	9333 (3)	−1451 (6)	63 (2)
C(18)	5693 (2)	8872 (3)	2009 (5)	60 (1)
C(19)	5252 (3)	6877 (4)	2226 (5)	61 (2)
C(20)	5311 (3)	6122 (3)	−1143 (7)	62 (2)
C(21)	5878 (3)	7613 (4)	−3418 (4)	60 (1)

[a] Equivalent isotropic *U* defined as one-third of the trace of the orthogonalized U_{ij} tensor.

Table VII. Selected Bond Distances and Angles for Cp*Rh{η^5-C_4Me_4Fe(CO)$_3$}

	Bond Distances (Å)		
Rh-Fe	2.563 (1)	Rh-C(5)	2.187 (3)
Rh-CNT[a]	1.836 (3)	Fe-C(1)	1.787 (4)
Rh-C(4)	2.154 (3)	Rh-C(6)	2.178 (3)
Rh-C(7)	2.161 (3)	Fe-C(4)	1.972 (3)
Fe-C(7)	1.974 (3)	C(7)-C(6)	1.428 (5)
C(6)-C(5)	1.433 (4)	C(5)-C(4)	1.419 (4)
Fe-C(3)	1.789 (4)	Fe-C(2)	1.769 (4)
	Bond Angles (deg)		
CNT-Rh-Fe	136.1 (1)	C(5)-C(6)-C(7)	113.2 (3)
CNT-Rh-C(4)	142.8 (1)	C(4)-Rh-Fe	48.5 (1)
CNT-Rh-C(5)	145.6 (1)	Fe-Rh-C(5)	74.3 (1)
CNT-Rh-C(6)	144.8 (1)	Fe-Rh-C(6)	74.7 (1)
CNT-Rh-C(3)	142.1 (1)	Fe-Rh-C(7)	48.5 (1)
Rh-Fe-C(1)	105.7 (1)	C(1)-Fe-C(2)	101.3 (2)
Rh-Fe-C(2)	142.6 (1)	C(1)-Fe-C(3)	89.6 (2)
Rh-Fe-C(3)	105.4 (1)	Rh-Fe-C(4)	54.9 (1)
C(2)-Fe-C(3)	100.1 (2)	C(1)-Fe-C(4)	90.8 (1)
Rh-Fe-C(7)	55.1 (1)	C(3)-Fe-C(4)	159.5 (1)
C(2)-Fe-C(4)	54.9 (1)	C(2)-Fe-C(7)	97.9 (1)
C(1)-Fe-C(7)	160.3 (1)	Rh-C(4)-Fe	76.6 (1)
C(3)-Fe-C(7)	91.7 (1)	Rh-C(7)-Fe	76.4 (1)
C(4)-Fe-C(7)	81.1 (1)	C(6)-C(7)-Fe	115.4 (2)
Fe-C(4)-C(5)	115.5 (2)	Fe-C(4)-C(8)	125.5 (2)
C(4)-C(5)-C(6)	113.7 (3)	Fe-C(7)-C(11)	125.3 (2)

[a] CNT = centroid of Cp* ring.

Absorption corrections were applied to the data set with maximum and minimum transmission factors of 0.739 and 0.679, respectively. The structure was solved by direct methods (SHELXS-86). Correct positions for Fe and Rh atoms were deduced from an *E* map. Subsequent least-squares difference Fourier calculations revealed positions for the remaining non-hydrogen atoms. Hydrogen atoms were included as fixed contributors in the "idealized" positions. In the final cycle of least-squares refinement, anisotropic thermal coefficients were refined for non-hydrogen atomsand a common isotropic thermal parameter was varied for hydrogen atoms. Successful convergence was indicated by the maximum shift/error for the last cycle. The final difference Fourier map had no significant features. A final analysis of variance between observed and calculated structure factors revealed no apparent systematic errors. Crystal, data collection, and refinement parameters are listed in Table III. Atomic coordinates and isotropic thermal parameters are listed in Table VIII. Selected bond distances and angles are listed in Table IX.

Table VIII. Atomic Coordinates and Isotropic Thermal Parameters (Å^2 × 10^3) for (Cp*Rh)$_2$(μ-CO)(μ_3-S)Fe(CO)$_3$

	x	*y*	*z*	*U*
Rh1	0.13023 (4)	0.35932 (3)	0.21054 (3)	31.5 (3)
Rh2	−0.02492 (4)	0.26889 (3)	0.28509 (3)	30.4 (3)
Fe	0.00973 (8)	0.22594 (6)	0.12211 (5)	46.9 (5)
S	0.1329 (1)	0.2089 (1)	0.2435 (1)	36.5 (8)
O1	−0.0812 (6)	0.0403 (4)	0.1053 (5)	137 (6)
O2	−0.1936 (6)	0.3043 (5)	0.0170 (4)	86 (5)
O3	0.1481 (6)	0.2211 (5)	−0.0196 (4)	116 (5)
O4	−0.1050 (4)	0.4326 (3)	0.1780 (3)	48 (3)
C1	−0.0457 (7)	0.1127 (5)	0.1128 (5)	74 (5)
C2	−0.1117 (7)	0.2748 (5)	0.0587 (5)	61 (6)
C3	0.0935 (7)	0.2240 (5)	0.0363 (5)	73 (5)
C4	−0.0378 (5)	0.3759 (4)	0.2022 (4)	39 (3)
C5	0.2164 (6)	0.4817 (5)	0.2659 (4)	77 (5)
C6	0.1670 (5)	0.5048 (4)	0.1854 (4)	49 (4)
C7	0.2221 (5)	0.4503 (4)	0.1284 (4)	44 (3)
C8	0.3000 (5)	0.3926 (4)	0.1832 (4)	33 (3)
C9	0.2975 (6)	0.4133 (5)	0.2731 (4)	55 (5)
C10	0.1855 (9)	0.5280 (6)	0.3586 (6)	200 (10)
C11	0.0837 (7)	0.5787 (5)	0.1583 (7)	75 (6)
C12	0.2060 (7)	0.4561 (6)	0.0282 (4)	108 (6)
C13	0.3811 (6)	0.3266 (6)	0.1483 (6)	44 (5)
C14	0.3721 (8)	0.3711 (6)	0.3538 (5)	121 (8)
C15	−0.0394 (5)	0.2787 (4)	0.4308 (4)	44 (4)
C16	−0.0494 (6)	0.1878 (5)	0.4040 (4)	73 (5)
C17	−0.1497 (7)	0.1809 (6)	0.3343 (5)	85 (6)
C18	−0.1953 (6)	0.2704 (6)	0.3222 (4)	39 (4)
C19	−0.1273 (6)	0.3292 (5)	0.3793 (4)	55 (4)
C20	0.0485 (7)	0.3176 (6)	0.5048 (4)	80 (5)
C21	0.0262 (9)	0.1103 (6)	0.4435 (7)	166 (10)
C22	−0.196 (1)	0.0931 (8)	0.2959 (7)	250 (20)
C23	−0.3034 (7)	0.2978 (10)	0.2611 (6)	36 (4)
C24	−0.1495 (8)	0.4303 (6)	0.3910 (5)	145 (9)

Table IX. Selected Bond Distances and Angles for (Cp*Rh)$_2$(μ-CO)(μ_3-S)Fe(CO)$_3$

	Distances (Å)		
Rh1-Rh2	2.6811 (7)	Rh1-Fe	2.6646 (10)
Rh2-Fe	2.6470 (9)	Rh1-S	2.266 (2)
Rh2-S	2.269 (2)	Fe-S	2.179 (8)
Fe-C1	1.789 (8)	Fe-C2	1.762 (8)
Fe-C3	1.768 (8)	Rh1-C4	2.013 (6)
Rh2-C4	2.004 (6)		
	Angles (deg)		
Rh2-Rh1-Fe	59.36 (2)	Rh2-Rh1-S	53.80 (4)
Fe-Rh1-S	51.68 (5)	Rh1-Rh2-Fe	60.01 (2)
Rh1-Rh2-S	53.70 (4)	Fe-Rh2-S	51.92 (5)
Rh1-Fe-Rh2	60.63 (2)	Rh1-Fe-S	54.67 (4)
Rh2-Fe-S	55.05 (5)	Rh1-S-Rh2	72.50 (5)
Rh1-S-Fe	73.65 (5)	Rh2-S-Fe	73.02 (5)
Rh1-C4-Rh2	83.8 (2)		

Acknowledgment. This research was supported by the National Science Foundation and the Department of Energy. We thank Johnson Matthey for the loan of rhodium trichloride. Jinling Hao assisted in the synthesis of 3,4-bis(chloromethyl)-2,5-dimethylthiophene, and Anton Skaugset collaborated in the synthesis of **1**.

Supplementary Material Available: Tables of bond angles and distances and positional and thermal parameters for compounds 2–4 (16 pages); structure factor tables (56 pages). Ordering information is given on any current masthead page.